HAL
open science

In-flight distribution of an electron within a surface acoustic wave

Hermann Edlbauer, Junliang Wang, Shunsuke Ota, Aymeric Richard, Baptiste Jadot, Pierre-André Mortemousque, Yuma Okazaki, Shuji Nakamura, Tetsuo Kodera, Nobu-Hisa Kaneko, et al.

To cite this version:

Hermann Edlbauer, Junliang Wang, Shunsuke Ota, Aymeric Richard, Baptiste Jadot, et al.. In-flight distribution of an electron within a surface acoustic wave. Applied Physics Letters, 2021, 119 (11), pp.114004. 10.1063/5.0062491 . hal-03372308

HAL Id: hal-03372308

https://hal.science/hal-03372308v1

Submitted on 25 Aug 2023

HAL is a multi-disciplinary open access archive for the deposit and dissemination of scientific research documents, whether they are published or not. The documents may come from teaching and research institutions in France or abroad, or from public or private research centers.

L'archive ouverte pluridisciplinaire **HAL**, est destinée au dépôt et à la diffusion de documents scientifiques de niveau recherche, publiés ou non, émanant des établissements d'enseignement et de recherche français ou étrangers, des laboratoires publics ou privés.

Applied Physics Letters ARTICLE scitation.org/journal/apl

In-flight distribution of an electron within a surface acoustic wave

Cite as: Appl. Phys. Lett. **119**, 114004 (2021); doi: 10.1063/5.0062491
Submitted: 6 July 2021 · Accepted: 20 August 2021 ·
Published Online: 14 September 2021

View Online Export Citation CrossMark

Hermann Edlbauer,[1] Junliang Wang,[1] Shunsuke Ota,[2,3] Aymeric Richard,[1] Baptiste Jadot,[1,4] Pierre-André Mortemousque,[1,4] Yuma Okazaki,[3] Shuji Nakamura,[3] Tetsuo Kodera,[2] Nobu-Hisa Kaneko,[3] Arne Ludwig,[5] Andreas D. Wieck,[5] Matias Urdampilleta,[1] Tristan Meunier,[1] Christopher Bäuerle,[1] and Shintaro Takada[3,a)]

AFFILIATIONS

[1]University Grenoble Alpes, CNRS, Grenoble INP, Institut Néel, 38000 Grenoble, France
[2]Department of Electrical and Electronic Engineering, Tokyo Institute of Technology, Tokyo 152-8550, Japan
[3]National Institute of Advanced Industrial Science and Technology (AIST), National Metrology Institute of Japan (NMIJ), 1-1-1 Umezono, Tsukuba, Ibaraki 305-8563, Japan
[4]University Grenoble Alpes, CEA, Leti, F-38000 Grenoble, France
[5]Lehrstuhl für Angewandte Festkörperphysik, Ruhr-Universität Bochum Universitätsstraße 150, 44780 Bochum, Germany

[a)]Author to whom correspondence should be addressed: shintaro.takada@aist.go.jp

25 August 2023 12:43:46

ABSTRACT

Surface acoustic waves (SAWs) have large potential to realize quantum-optics-like experiments with single flying electrons employing their spin or charge degree of freedom. For such quantum applications, highly efficient trapping of the electron in a specific moving quantum dot (QD) of a SAW train plays a key role. Probabilistic transport over multiple moving minima would cause uncertainty in synchronization that is detrimental for coherence of entangled flying electrons and in-flight quantum operations. It is thus of central importance to identify the device parameters enabling electron transport within a single SAW minimum. A detailed experimental investigation of this aspect is so far missing. Here, we fill this gap by demonstrating time-of-flight measurements for a single electron that is transported via a SAW train between distant stationary QDs. Our measurements reveal the in-flight distribution of the electron within the moving acousto-electric quantum dots of the SAW train. Increasing the acousto-electric amplitude, we observe the threshold necessary to confine the flying electron at a specific, deliberately chosen SAW minimum. Investigating the effect of a barrier along the transport channel, we also benchmark the robustness of SAW-driven electron transport against stationary potential variations. Our results pave the way for highly controlled transport of electron qubits in a SAW-driven platform for quantum experiments.

Published under an exclusive license by AIP Publishing. https://doi.org/10.1063/5.0062491

The use of sound enables nanoelectronic implementations that often resemble quantum-optics experiments within an original acousto-electric solid-state framework. A prominent example of this development is surface-acoustic-wave (SAW) technology, which is well-established in consumer-electronics industry and currently celebrates its revival in quantum science.[1–3] The acousto-electric medium can serve, for instance, as a resonator[4–6] or as a messenger[7,8] of quantum information from superconducting qubits. However, a SAW can also be employed to transport a charged quantum system as a whole what is particularly interesting for semiconductor-qubit architectures[9] and experimental investigations of quantum nonlocality with Fermions.[10] The acousto-electric potential modulation of the SAW drags a single electron with its quantum properties from one surface-gate defined quantum dot (QD) through a transport channel to another QD.[11–13] The SAW-driven transport technique allows high transfer efficiency $P > 99\%$ even in single-electron circuits of coupled transport channels.[14] Owing to this robustness, the acousto-electric method is capable of shuttling spin-entangled electron pairs between distant QDs without significant additional decoherence.[15] The exact transport process remains, however, an aspect that is yet not fully understood: Is the electron loosely surfing on a shallow potential wave or is it well-confined within a specific location of the wave train?

To study the physics of electron-transfer techniques, time-resolved measurements have emerged as a useful and reliable tool.[16] In the quantum-Hall regime, fast voltage-pulse probing has been employed to study the interaction of edge states[17] and it was applied to

Published under an exclusive license by AIP Publishing

demonstrate the dynamics of single electrons emitted from a QD pump.[18] Recently, time-of-flight measurements have been performed in a similar manner in non-chiral mesoscopic conductors.[19] For SAW-driven single-electron transport, pulsing techniques have been proposed[11] and were applied to trigger single-electron transport at a specific location of the acousto-electric wave train.[14,15] However, detailed time-of-flight measurements have not yet been performed.

Here, we present a pulse-probe technique that allows the measurement of the electrons in-flight distribution as it passes with the SAW at a specific point of a transport channel. To perform the time-of-flight measurement, we first apply a ps-voltage pulse to the reservoir gate (R) of the source QD, which allows us to load the electron into a specific SAW minimum. Subsequently, we apply another ps-pulse on a barrier gate (#1 or #2) that is placed along the transport channel as the SAW train passes with the flying electron. Sweeping the delay of this probe event, we scan the presence of the electron and map its in-flight distribution for each SAW minimum. By changing the acousto-electric amplitude, we estimate the threshold necessary to confine the electron in the initially loaded SAW minimum. Introducing a local surface-gate controlled barrier along the transport channel, we investigate further the effect of a stationary potential variation on the in-flight distribution and compare the experimental results to potential simulations. The present time-resolved investigation provides an important benchmark for the acousto-electric amplitude and the potential homogeneity that is required to perform robust SAW-driven qubit transport and in-flight quantum operations.

The experiment is performed at a temperature of about 20 mK within a ^{3}He/^{4}He dilution refrigerator. A Si-modulation-doped GaAs/AlGaAs heterostructure serves as basis of the investigated sample that is schematically shown in Fig. 1(a). The two-dimensional electron gas (2DEG) that is located 110 nm below the surface has an electron density of $n \approx 2.8 \times 10^{-11}\,\mathrm{cm}^{-2}$ and a mobility of $\mu \approx 9 \times 10^5\,\mathrm{cm}^2\,\mathrm{V}^{-1}\,\mathrm{s}^{-1}$. The main component of the sample is a surface-gate-defined transport channel, whose ends are equipped with a quantum dot (QD) serving as a single-electron source and a receiver. A scanning-electron-microscopy (SEM) image of the transport channel is shown in Fig. 1(b) with schematics indicating the experimental setup. The Schottky gates of the nanostructure are made out of a metal stack of 3 nm titanium and 14 nm gold. During the cooldown, a voltage of 0.3 V is applied to all electrodes. At low temperatures, we completely deplete the 2DEG lying below the 20 μm-long transport channel and control the source and receiver QD via a set of negative voltages. The occupation of each QD is sensed via the current flowing through an adjacent quantum point contact (QPC).

An interdigital transducer (IDT) is placed far to the left of the nanostructure, which allows single-shot emission of a SAW train—with 1 μm wavelength—that propagates with a speed of $v_{\mathrm{SAW}} \approx 2.86\,\mu$m/ns toward the transport channel.[20] The input signal for the IDT stems from an output channel of an arbitrary waveform generator (AWG). In order to shuttle a single electron from one QD to the other, we employ the potential modulation that accompanies the SAW in the piezoelectric substrate. At the depleted transport channel, this acousto-electric modulation forms a train of potential minima that is capable to move the electron. We trigger the SAW-driven sending event via the reservoir gate (R) of the source QD that is connected to an AWG output. To carry out the time-of-flight measurement, additionally, two barriers (#1 and #2) are placed along the channel, which are also linked to AWG outputs. Details of the employed IDT and the microwave setup are provided in the supplementary material, Sects. 1 and 2.

Before the emission of the SAW train, an electron is loaded at the source QD and prepared in a protected configuration where the acousto-electric wave cannot pickup the electron. In this sending configuration, a slight potential variation is however sufficient to move the electron from the stationary source QD into one of the moving QDs that accompanies the SAW train along the transport channel—see red schematic in Fig. 1(c). At the same time, we prepare the receiver quantum dot in a configuration, where we can catch the moving electron. Details of the calibration of the SAW-driven transport procedure are provided in the supplementary material, Sec. 3. Figure 1(d) shows the transfer probability as a function of the source-pulse delay, t_{S}. As in previous investigations,[14] we find that t_{S} must coincide with a specific acousto-electric pressure phase of the SAW in order to enable the electron's transfer from the stationary source QD into a specific location within the SAW.

To perform the time-of-flight measurement, we fix the timing of the sending trigger ($t_{\mathrm{S}} = 0$ ns) and sweep the delay of a probe pulse t at the according barrier over the arrival window of the SAW. We have chosen the probe-pulse width as two fifths of the SAW period T_{SAW} in order to optimize the pulsing efficiency and time resolution. The delay of the probe pulse is stepped in multiples of the period T_{SAW} with a time offset enabling coincidence with the pressure phase of the SAW. If the probe pulse overlaps with a certain SAW minimum, it enables, thus, a potentially present electron to pass. Otherwise, the passage of the electron is blocked, leaving the electron behind the barrier in the subsequent SAW period. Let us first consider the hypothetical case, where the electron is well-confined in a specific SAW minimum. In this case, the transfer probability is zero for a barrier-pulse delay before the electron arrival. For any delay in the pressure phase after the arrival, the electron is on the other hand certainly transmitted, since it is blocked before the barrier until the probe pulse is present. Following this measurement approach, the instantaneous distribution of the electron within the passing SAW train, $D(t)$, is directly reflected via the derivative of the transfer probability, P, with respect to the time delay, t, of the probe pulse if the effect of the barrier pulse is fully deterministic (block or transmit). We estimate the uncertainty in $D(t)$ via error propagation as approximately three times the error of $P = 1/\sqrt{N}$, where N indicates the number of single-shot transfers. For a deterministic probe pulse and single-minimum transport, $D(t)$ should follow a delta function at the SAW location expected from the triggered sending event (t_{S}).

Let us first perform the time-of-flight measurement at the maximum achievable IDT input power of about 288 mW (24.6 dBm). Based on SAW-modulated Coulomb-peak data[14,21]—see the supplementary material, Sec. 4—we estimate that this input power introduces a SAW with amplitude $A_{\mathrm{SAW}} \approx (24 \pm 3)$ meV. We estimate the expected arrival time (t_1) at barrier #1 from its distance to the source QD (x_1) as $t_1 = x_1/v_{\mathrm{SAW}} \approx (2.23 \pm 0.05)$ ns. Sweeping the delay of the probe pulse on barrier #1 over the time window around t_1, we measure the transfer probability $P(t)$ as shown in Fig. 2(a). The data follow a step function that is centered at t_1 what verifies the deterministic effect of the barrier pulse and transport in a specific SAW position. It is important to note that the binary probing process is achieved

25 August 2023 12:43:46

Published under an exclusive license by AIP Publishing

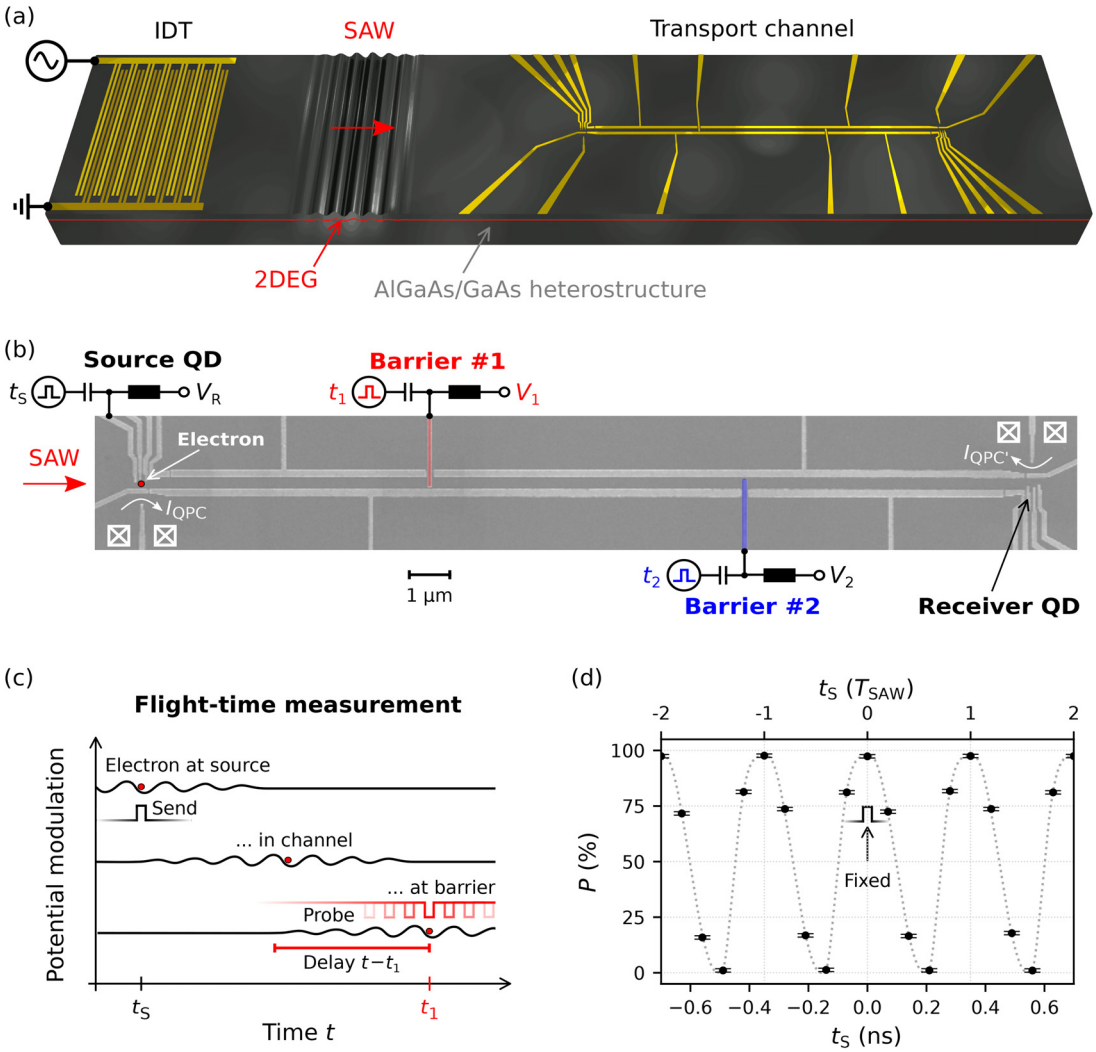

FIG. 1. Experimental setup. (a) Schematic of the AlGaAs/GaAs sample showing an interdigital transducer (IDT) that launches a SAW train toward the surface-gate defined transport channel. (b) SEM image of transport channel showing source and receiver quantum dots (QDs) with schematic indication of quantum-point-contact (QPC) charge detectors and the voltage-pulse to perform the time-of-flight measurement. (c) Schematics showing principles of the controlled sending process at the source and the principle of the time-of-flight measurement. (d) Transfer probability, P, as a function of the sending pulse t_S. The probability values P are obtained from $N = 13\,000$ single-shot transmissions with error $\Delta P = 1/\sqrt{N}$. The dotted line serves as guide to the eye. The arrow indicates the delay of the sending pulse that is kept fixed for the time-of-flight measurements.

via the sample design, allowing a spatial separation of the probing barrier to the catching event at the receiver QD. Evaluating the electron distribution $D(t)$, we find that the electron is confined during transport with a certainty of $(97 \pm 2)\%$ at the position of the SAW train $(t - t_1 = 0)$, where the electron was initially loaded with the ps-voltage pulse. We suspect that even more confinement is achievable if the SAW amplitude would be further increased.

In order to investigate this aspect in more detail, let us focus on the threshold of the SAW amplitude below which confinement breaks down. For this purpose, we repeat the time-of-flight measurement at the first barrier with gradually decreasing SAW amplitude as shown in Fig. 2(b). At a SAW amplitude of about 19 meV, we observe partial electron arrival one SAW minimum earlier than expected $(t - t_1 = -T_{SAW})$. For a SAW amplitude below 15 meV, we find the arrival distribution also spreading over SAW minima subsequent to the expected location. We quantify the magnitude of electron displacement by plotting $D_0 = D(t_1)$ as a function of the SAW amplitude as shown in Fig. 2(c). The data show significant $(D_0 > 95\%)$ in-flight confinement of the transported electron for a SAW amplitude exceeding a threshold of (24 ± 3) meV. The course of the data indicates that increased SAW amplitude, indeed, allows maximization of in-flight confinement.

The presence of two controllable barriers along the transport channel allows us to study the effect of an intermediate potential variation on the time-of-flight distribution. For this purpose, we probe the

25 August 2023 12:43:46

Published under an exclusive license by AIP Publishing

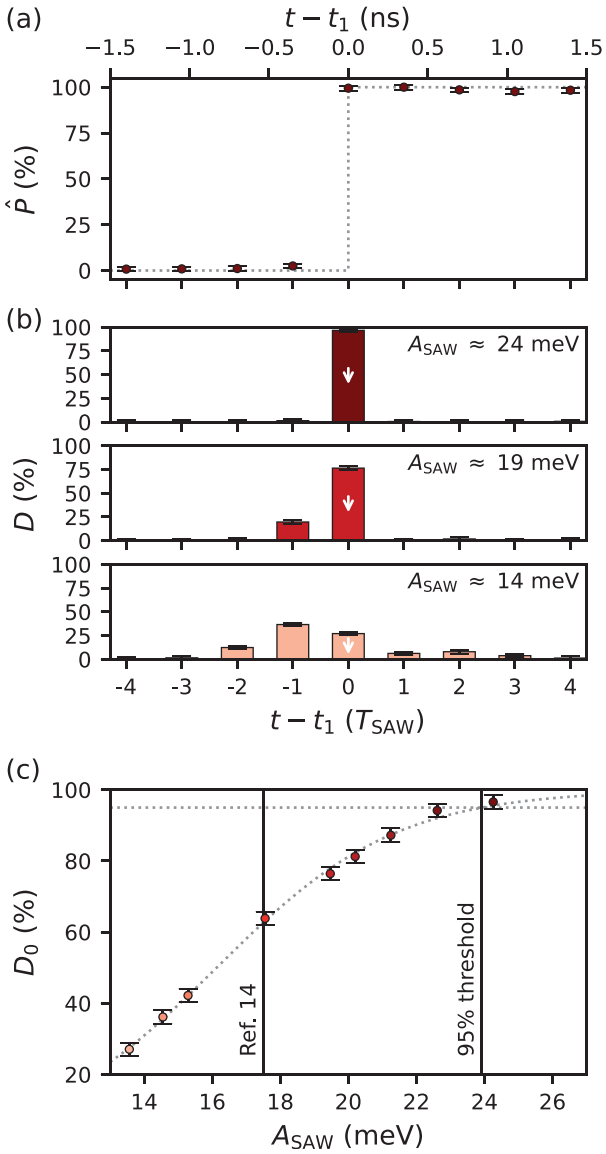

FIG. 2. Time-of-flight measurement at barrier #1. (a) Normalized transfer efficiency $\hat{P}$ as a function of delay on the probe pulse t. Each data point is derived from $N = 25\,000$ single-shot transmissions with error $\Delta P = 1/\sqrt{N}$. The dotted line shows a step function centered at the expected arrival time t_1. (b) In-flight distribution $D(t)$ of the electron within the SAW train for different values of the peak-to-peak SAW amplitude A_{SAW}. The data are obtained via the normalized derivative of $P(t)$ with uncertainty $\Delta D \approx 3\Delta P$. The arrows indicate the confinement fidelity $D_0 = D(t_1)$. (c) D_0 as a function of the SAW amplitude A_{SAW}. The correspondence between the SAW amplitude and the input power is provided in the supplementary material, section 4. The dotted curves show a guide to the eye (sigmoid function) and the 95% threshold. The two vertical lines indicate the SAW amplitude employed in a previous work[14] and the amplitude for significant confinement.

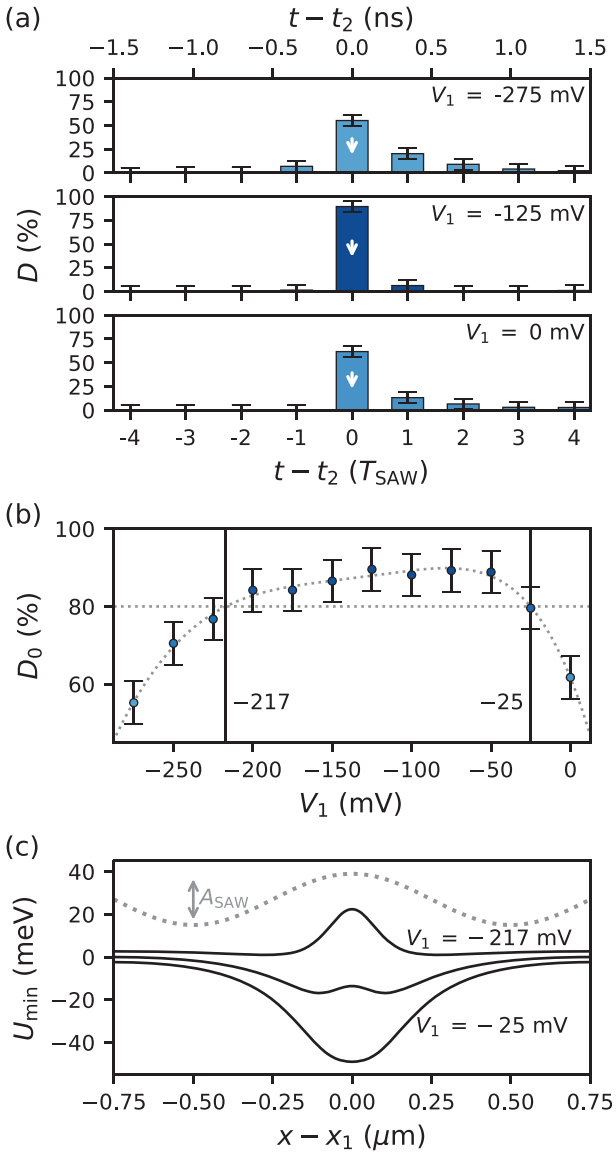

FIG. 3. Time-of-flight measurement at barrier #2. (a) In-flight distribution $D(t)$ of the electron within the SAW-train for selected voltages V_1 applied on the first barrier gate. The measurement is performed with the maximum SAW amplitude of about 24 meV. Each data point is derived from $N = 3000$ single-shot transmissions with uncertainty $\Delta D \approx 3/\sqrt{N}$. (b) Confinement fidelity $D_0 = D(t_1)$ for different values of V_1. The dotted curves show a guide to the eye (polynomial fit) and the 80% threshold. (c) Minimum U_{min} of the electron potential across the first barrier of three selected voltages: −217, −121, and −25 mV. The dotted curve shows the potential modulation of the applied SAW for comparison with indication of its peak-to-peak amplitude A_{SAW}.

electron's arrival at the second barrier. There, we expect the electrons' passage at a time of $t_2 = x_2/v_{SAW} \approx (4.86 \pm 0.05)$ ns, where x_2 indicates the distance of barrier #2 to the source QD. On the first barrier we do not apply a voltage pulse, but only change the static voltage V_1. Figure 3(a) shows data of such a time-of-flight measurement with an intermediate barrier. Here, we keep the SAW amplitude at the maximum achievable value. Despite the presence of the intermediate barrier, the data show a confinement fidelity $D_0 > 80\%$ in the voltage range between −217 and −25 mV. Beyond this range, we observe a

25 August 2023 12:43:46

Published under an exclusive license by AIP Publishing

rapid drop of D_0 due to in-flight transitions of the electron in neighboring SAW minima. The presence of the intermediate barrier causes a reduction in the confinement fidelity compared to a smooth potential along the transport channel.

To understand the experimental result better, let us compare the time-of-flight data to potential simulations along the transport channel. The potential calculation is performed via the commercial Poisson solver nextnano[23] assuming a frozen charge layer and deep boundary conditions.[24] As input parameters, we consider the gate geometry and the voltages applied as well as the intrinsic properties of the heterostructure. Figure 3(c) shows the course of the resulting potential minimum $U_{\min}$ across the first barrier for three values of the voltage V_1 beyond the 80%-confinement threshold. The blockade of the electron for a very high ($V_1 < -217\,\mathrm{mV}$) and very low ($V_1 > -25\,\mathrm{mV}$) potential barrier is caused by different effects. For increasingly negative barrier voltages, a potential barrier is formed. Interestingly, the formation of the barrier comes along with the event, where the electron arrives one SAW minimum earlier as apparent in Fig. 3(a) for $V_1 = -275\,\mathrm{mV}$ at $t - t_2 = -1T_{\mathrm{SAW}}$. We speculate that the advancement is caused via non-adiabatic transitions of the electron in excited states when ramping against the barrier. For increasingly positive voltages such as $V_1 = 0\,\mathrm{mV}$, we observe on the other hand mainly transitions in subsequent SAW minima ($t - t_2 > 0$) due to trapping in a quantum-dot like potential structure. The time-of-flight measurement at the second barrier shows that single-minimum transport is feasible even if significant potential gaps are present along the transport channel. We suspect that maximized acousto-electric confinement (via increased SAW-amplitude and -frequency) enables single-electron transfer that is fully protected against local potential variations.[22]

The ability to detect the exact location of a SAW-transported electron is essential to identify the critical device parameters enabling single-electron transport within a specific, deliberately chosen SAW minimum and, thus, flying-qubit implementations. Employing a pulse-probe technique, we have demonstrated time-of-flight measurements revealing the arrival distribution of such a flying electron for each moving potential minima that accompanies the SAW along a transport channel. As we send a SAW train with sufficiently large peak-to-peak amplitude—that is $(24 \pm 3)\,\mathrm{meV}$ for the presently investigated device—the time-of-flight data indicate an electron-confinement fidelity exceeding 95% within a specific moving QD. Investigating the effect of an intermediate surface-gate-defined barrier within the transport channel, we demonstrate a confinement fidelity larger than 80% over a voltage range of about 200 mV despite the presence of the local potential variation. Our measurements show that acousto-electric in-flight confinement plays the key role to make a SAW-driven single-electron circuit robust. We anticipate that our experimental findings foster the development and application of SAW-generation approaches[25–30] paving the way for SAW-driven electron-quantum-optics implementations[31–34] and quantum-metrology applications.[35]

See the supplementary material for detailed description of (1) the IDT and the employed SAW signal, (2) the setup for the voltage pulses, (3) the single-electron-transport procedure, and (4) the estimation of the acousto-electric potential modulation.

AUTHORS' CONTRIBUTIONS

H.E., J.W., and S.O. contributed equally to this work.

J.W. acknowledges the European Union's Horizon 2020 research and innovation program under the Marie Skłodowska-Curie Grant Agreement No. 754303. T.K. and S.T. acknowledge financial support from JSPS KAKENHI Grant No. 20H02559. N.-H.K. acknowledges financial support from JSPS KAKENHI Grant No. JP18H05258. C.B. acknowledges funding from the European Union's H2020 research and innovation programme under Grant Agreement No. 862683.

DATA AVAILABILITY

The data that support the findings of this study are available from the corresponding author upon reasonable request.

REFERENCES

[1] C. J. B. Ford, "Transporting and manipulating single electrons in surface-acoustic-wave minima," Phys. Status Solidi B **254**, 1600658 (2017).
[2] C. Bäuerle, C. D. Glattli, T. Menuier *et al.*, "Coherent control of single electrons: A review of current progress," Rep. Prog. Phys. **81**, 056503 (2018).
[3] P. Delsing, A. N. Cleland, M. Schuetz *et al.*, "The 2019 surface acoustic waves roadmap," J. Phys. D **52**, 353001 (2019).
[4] M. V. Gustafsson, T. Aref, A. F. Kockum *et al.*, "Propagating phonons coupled to an artificial atom," Science **346**, 207–211 (2014).
[5] R. Manenti, A. F. Kockum, A. Patterson *et al.*, "Circuit quantum acoustodynamics with surface acoustic waves," Nat. Commun. **8**, 975 (2017).
[6] G. Andersson, B. Suri, L. Guo *et al.*, "Non-exponential decay of a giant artificial atom," Nat. Phys. **15**, 1123–1127 (2019).
[7] K. J. Satzinger, Y. P. Zhong, H. S. Chang *et al.*, "Quantum control of surface acoustic-wave phonons," Nature **563**, 661–665 (2018).
[8] A. Bienfait, K. J. Stazinger, Y. P. Zhong *et al.*, "Phonon-mediated quantum state transfer and remote qubit entanglement," Science **364**(6438), 368–371 (2019).
[9] L. M. K. Vandersypen, H. Bluhm, J. S. Clarke *et al.*, "Interfacing spin qubits in quantum dots and donors—hot, dense, and coherent," npj Quantum Inf. **3**, 34 (2017).
[10] A. Bertoni, P. Bordone, R. Brunetti *et al.*, "Quantum logic gates based on coherent electron transport in quantum wires," Phys. Rev. Lett. **84**, 5912–5915 (2000).
[11] S. Hermelin, S. Takada, M. Yamamoto *et al.*, "Electrons surfing on a sound wave as a platform for quantum optics with flying electrons," Nature **477**, 435 (2011).
[12] R. P. G. McNeil, M. Kataoka, C. J. B. Ford *et al.*, "On-demand single-electron transfer between distant quantum dots," Nature **477**, 439 (2011).
[13] B. Bertrand, S. Hermelin, S. Takada *et al.*, "Fast spin information transfer between distant quantum dots using individual electrons," Nat. Nanotechnol. **11**, 672 (2016).
[14] S. Takada, H. Edlbauer, H. Lepage *et al.*, "Sound-driven single-electron transfer in a circuit of coupled quantum rails," Nat. Commun. **10**, 4557 (2019).
[15] B. Jadot, P.-A. Mortemousque, E. Chanrion *et al.*, "Distant spin entanglement via fast and coherent electron shuttling," Nat. Nanotechnol. **16**, 570–575 (2021).
[16] G. Sukhodub, F. Hohls, and R. J. Haug, "Observation of an interedge magnetoplasmon mode in a degenerate two-dimensional electron gas," Phys. Rev. Lett. **93**, 196801 (2004).
[17] H. Kamata, N. Kumada, M. Hashisaka *et al.*, "Fractionalized wave packets from an artificial Tomonaga–Luttinger liquid," Nat. Nanotechnol. **9**, 177–181 (2014).
[18] M. Kataoka, N. Johnson, C. Emary *et al.*, "Time-of-flight measurements of single-electron wave packets in quantum hall edge states," Phys. Rev. Lett. **116**, 126803 (2016).
[19] G. Roussely, E. Arrighi, G. Giorgos *et al.*, " Unveiling the bosonic nature of an ultrashort few-electron pulse," Nat. Commun. **9**, 2811 (2018).
[20] The SAW wavelength λ_{SAW} is determined by the period of the metallic fingers of the IDT. For the presently investigated device the SAW wavelength is 1 μm. From the measured resonance frequency of the IDT, $f_0 = 2.86\,\mathrm{GHz}$, the SAW velocity is deduced from $v_{\mathrm{SAW}} = \lambda_{\mathrm{SAW}} f_0$.

25 August 2023 12:43:46

Published under an exclusive license by AIP Publishing

[21]R. J. Schneble, M. Kataoka, C. J. B. Ford *et al.*, "Quantum-dot thermometry of electron heating by surface acoustic waves," Appl. Phys. Lett **89**, 122104 (2006).
[22]J. A. Nixon and J. H. Davies, "Potential fluctuations in heterostructure devices," Phys. Rev. B **41**, 7929 (1990).
[23]S. Birner, T. Zibold, T. Andlauer *et al.*, "nextnano: General purpose 3-D simulations," IEEE Trans. Electron Devices **54**, 2137–2142 (2007).
[24]H. Hou, Y. Chung, G. Rughoobur *et al.*, "Experimental verification of electrostatic boundary conditions in gate-patterned quantum devices," J. Phys. D **51**, 244004 (2018).
[25]S. Büyükköse, B. Vratzov, D. Ataç *et al.*, "Ultrahigh-frequency surface acoustic wave transducers on $ZnO/SiO_2/Si$ using nanoimprint lithography," Nanotechnology **23**, 315303 (2012).
[26]E. D. S. Nysten, A. Rastelli, and H. J. Krenner, "A hybrid (Al)GaAs-$LiNbO_3$ surface acoustic wave resonator for cavity quantum dot optomechanics," Appl. Phys. Lett. **117**, 121106 (2020).
[27]M. K. Ekström, T. Aref, J. Runeson *et al.*, "Surface acoustic wave unidirectional transducers for quantum applications," Appl. Phys. Lett. **110**, 073105 (2017).
[28]É. Dumur, K. J. Satzinger, G. A. Peairs *et al.*, "Unidirectional distributed acoustic reflection transducers for quantum applications," Appl. Phys. Lett. **114**, 223501 (2019).
[29]F. J. R. Schülein, E. Zallo, P. Atkinson *et al.*, "Fourier synthesis of radiofrequency nanomechanical pulses with different shapes," Nat. Nanotechnol. **10**, 512 (2015).
[30]M. Weiß, A. L. Hörner, E. Zallo *et al.*, "Multiharmonic frequency-chirped transducers for surface-acoustic-wave optomechanics," Phys. Rev. Appl. **9**, 014004 (2018).
[31]C. H. W. Barnes, J. M. Shilton, and A. M. Robinson, "Quantum computation using electrons trapped by surface acoustic waves," Phys. Rev. B **62**, 8410–8419 (2000).
[32]D. R. M. Arvidsson-Shukur, H. V. Lepage, E. T. Owen *et al.*, "Protocol for fermionic positive-operator-valued measures," Phys. Rev. A **96**, 052305 (2017).
[33]H. V. Lepage, A. A. Lasek, D. R. M. Arvidsson-Shukur *et al.*, "Entanglement generation via power-of-swap operations between dynamic electron-spin qubits," Phys. Rev. A **101**, 022329 (2020).
[34]M. J. A. Schuetz, J. Knorzer, G. Giedke *et al.*, "Acoustic traps and lattices for electrons in semiconductors," Phys. Rev. X **7**, 041019 (2017).
[35]J. Cunningham, V. I. Talyanskii, J. M. Shilton *et al.*, "Quantized acoustoelectric current - An alternative route towards a standard of electric current," J. Low Temp. Phys. **118**, 555 (2000).

25 August 2023 12:43:46

Published under an exclusive license by AIP Publishing